Theoretical Study on the Antioxidant Activity of Nitrones as OH· Free Radical Trappers

*JOSÉ MUÑOZ- ESPINOZA[1,2 *], GERMÁN BARRIGA-GONZÁLEZ[2]*

1. Department of Chemistry, Faculty of Science, University of Chile, Santiago, Chile.
2. Department of Chemistry, Faculty of Basic Science, Metropolitan University of Education Sciences, Santiago, Chile

ABSTRACT

In the present article, a theoretical and computational study was carried out on the reactivity and antioxidant capacity of a series of nitrone derivatives (hBNn) in the presence of the OH· radical. For the antioxidant characterization of these compounds, tools such as global and local reactivity indices were used, as well as thermodynamic aspects to obtain the most energetically stable product. In addition, the NBO analysis, which described the SOMO generated by the electron radical of the spin adduct hBNn-OH. The results obtained show that the nitrone derivatives studied present the antioxidant capacity of radical trapping, forming energetically stable spin adducts. In turn, the reactivity of the systems (nitrone and radical) shows their nucleophilic and electrophilic tendencies, allowing us to propose a reaction mechanism for these radical traps.

Keywords: *Nitrones; Free Radicals; SOMO; Reactivity.*

1. INTRODUCTION

Free radicals are a type of chemical species (atom or molecule) that are highly reactive and have a short half-life due to the presence of unpaired electrons, which can cause damage at the cellular level and even DNA [1]. Among the best known pathologies produced by the action of free radicals (oxidative stress) are neurodegenerative disorders such as Alzheimer's [2,3] and Parkinson's [4,5,6], and somatic disorders such as cancer [7,8], hypertension [9], diabetes [10,11], and even aging.

Among the best known radicals are reactive oxygen species (ROS) (O_2, OH, RO_2·1) [12] and reactive nitrogen species (RNS) (·NO, ·NO_2) [13], which are generated by various metabolic mechanisms in cells such as mitochondrial oxidative phosphorylation (in the case of ROS) [14] and conversion of L - arginine to L - citrulline and nitric oxide (in the case of RNS) [15]. One of the most reactive ROS is OH· which greatly promotes lipid peroxidation of cell membranes [16].
The generation of this radical is possible through the transfer of an electron, which can be contributed by cations, mainly transition metals such as Fe^{2+}, Cu^{+} or Mn^{+2}. The best-known reaction is the Fenton mechanism [17], which from the oxidetion of Fe^{2+}(or Cu^{+}) promoted by H_2O_2 produces the OH· radical.
Eq. 1:

$$Fe^{2+} + H_2O_2 \longrightarrow Fe^{3+} + OH^- + OH\cdot$$
$$Cu^{+} + H_2O_2 \longrightarrow Cu^{2+} + OH^- + OH\cdot$$

To combat free radicals, cells present endogenous protection mechanisms, mainly of the enzymatic type, such as superoxide dismutase (SOD), glutathione peroxidase (GSH-Px) and catalase (CAT) [18,19,20]. But to complement the antioxidant activity, there are exogenous antioxidants, such as vitamins (vitamin A and E), carotenoids (lycopene and β-carotene), flavones and polyphenols, which can be supplied by the diet [21]. These chemical compounds exhibit antioxidant activity through different mechanisms, as it depends on the structural nature of the molecule and the type of radical. Mainly, antioxidant mechanisms can be classified into HAT (Hydrogen Atom Transfer), SET (Single Electron Transfer) or SPLET (Sequential Proton Loss Electron Transfer) [22,23]. However, there are molecules with antioxidant property of the "radical trapping" type, which when interacting with free radicals, form spin adducts, which are less reactive and harmless radical species [24,25].

One of the nitro compounds that exhibit radical trapping activity are nitrones, specifically *α-phenyl-N-tert-butylnitrone* (PBN) [26,27], which thanks to this property have been shown to have neuroprotective activity [28].

Figure 1. Nitrone PBN and its derivatives Bisnitrones.

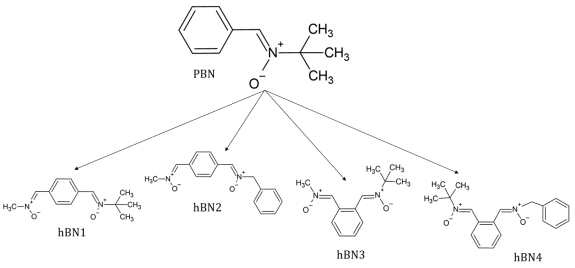

Diez et al. [27] carried out an experimental study on a new series of PBN nitrone derivatives (Figure 1) and their antioxidant properties, so that, by way of completeness, the present article aims to describe from the theoretical point of view the antioxidant mechanism as radical scavengers with the OH· radical. This description was carried out from the local reactivity indices such as Fukui functions ($f_{(r)}$) [29] and Dual Descriptor ($f^{(2)}$) [30] and global reactivity indices, while the radical electron distribution of the spin adduct can be modeled from the NBO (Natural Bond Orbital) model [31].

2. COMPUTATIONAL DETAILS

2.1 Design and Optimization of Nitrone Derivatives

For the design and construction of the Nitronas derivatives, the GaussView 5.0.9 software was used, while the geometric optimizations were performed in Gaussian '09 revision E.01 [32], using the Density Functional Theory (DFT) method with the functional and the basic set B3LYP/6-31+G(d,p).

**Corresponding author email:* jose.munoz.e@ug.uchile.cl

2.2. Spin Adducts and Transition State

The spin adducts were obtained from thermodynamic analysis of the system (frequency) and the local reactivity indices of the nitrones. The optimal spin adduct was considered as the one that presented a lower relative energy compared to the initial hBNn/OH· system, like the procedure presented by Allodi et al. [33]. To obtain the transition state, the QST2 method was used, which uses the optimized structures of the reactants (hBNn/OH·) and products (hBNn-OH), in which care must be taken with the enumerations of the atoms, since the calculation can collapse as there is not coherence in the reaction coordinates. To confirm the transition state, its imaginary frequency was considered [34].

2.3. Global and Local Reactivity Indices

The global and local reactivity indices of nitrone derivatives (hBNn) and the OH· radical were obtained through Fukui 4.1 Software [30,35,36] compatible with Gaussian '09. The calculation was performed through a singlepoint (SP) in Gaussian '09, considering the B3LYP/6-31G^{+}(d,p) functional and basis set.

The Fukui frontier molecular orbitals (FMO) approximation [29, 37,38] was used to plot the local descriptors, which were visualized in Gauss View generating isosurfaces of density 0.002 u. a.

2.4. Natural Bond Orbital (NBO)

To describe the presence of the radical electron in the spin adducts, the Natural Bond Orbital (NBO) model was used, which from its Lewis-type analysis provides a detailed picture of how the molecular orbitals are composed, which can be decomposed into bonding, non-bonding and anti-bonding orbitals [39]. This analysis was performed using the NBO 6.0 software [40], which uses the Gaussian.47 file as input. To obtain it, a singlepoint (SP) was performed considering the unrestricted state (UB3LYP/6-31G+(d,p)) which is useful for systems with unpaired electrons. For the visualization of the NBOs, Chemcraft software [41] was used.

Figure 2. Derivatives of hBNn nitrones (Bisnitrones) optimized in DFT B3LYP/6-31G+(d,p).

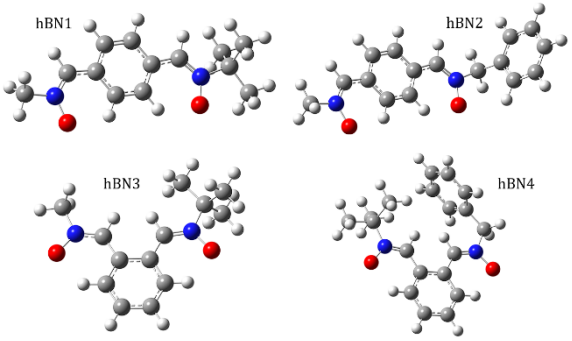

3. RESULT AND DISCUSSION

3.1. Optimized hBNn Nitrone Derivatives and Spin Adducts

The PBNn nitrone derivatives modeled and optimized from DFT with the B3LYP/6-31G+(d,p) functional and basis set, can be visualized in Figure 2

The Spin Adduct generated between the interaction of Bisnitronas (hBNn) and the OH· radical was obtained from the thermodynamic parameters (relative energy, enthalpy and Gibbs free energy) and the local reactivity indices, the latter being in charge of describing the site susceptible to react with the radical. Table 1 shows the thermodynamic values of the spin adducts and the transition state (TS) obtained from the QST2 method.

Table 1. Thermodynamic Parameters on Spin Adduct Formation

System	E/ (kcal/ mol)	H/ (kcal/ mol)	G/ (kcal/ mol)	System	E/ (kcal/ mol)	H/ (kcal/ mol)	g/ (kcal/ mol)
hBN1 /OH ·	-20.49	-20.46	-20.46	hBN3 /OH ·	-20.47	-20.46	-20.46
[hBN1 − OH ·]‡	-20.32	-20.31	-20.32	[hBN3 − OH ·]‡	-20.29	-20.26	-20.29
hBN1 − OH	-21.79	-21.78	-21.78	hBN3 − OH	-21.02	-21.03	-21.06
hBN2 /OH ·	-21.87	-21.86	-21.87	hBN4 /OH ·	-23.34	-23.33	-23.34
[hBN2 − OH ·]‡	-21.53	-21.52	-21.53	[hBN4 − OH ·]‡	-22.53	-22.53	-22.54
hBN2 − OH	-21.94	-21.93	-21.93	hBN4 − OH	-23.90	-23.89	-23.89

The thermodynamic parameters on the formation of the spin adduct (hBNn-OH) and the transition state ([hBNn-OH·]≠) can be seen graphically in Figure 3, where the energy barrier between reactants and transition state is relatively low. In turn, it can be observed that the relative energy of the reactants is considerably high compared to the products (spin adduct), which describes a highly stable system [34]. The hBN4-OH system being the most energetically stable.

Figure 3. Spin adduct formation process and transition state between hBNn nitrone derivative and OH· radical.

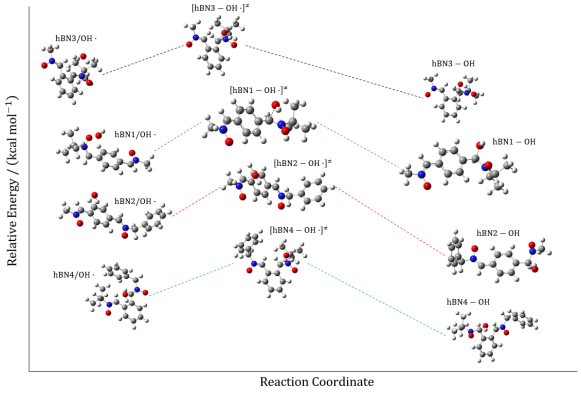

Although steric hindrance largely governs molecular reactions [42], it can be observed that, in this particular case, structures (spin adducts) are formed in which the radical attack is on the carbon atoms neighboring bulky groups (tert-butyl and benzyl), forming energetically stable products.

3.2. Global and Local Reactivity Indices

The reactivity of a chemical species can be described globally and locally [29], the global reactivity indices being mainly the chemical potential (μ), chemical hardness (η) and electrophilicity (ω^+) [43,44], while the local reactivity indices are the Fukui functions [29] and the dual descriptor [30]. All reactivity indices present in Table 2 were calculated from the following equations:

Eq. 2:

$$\mu = \left(\frac{\partial E}{\partial N}\right)_{v_{(r)}} \quad ; \quad \eta = \left(\frac{\partial \mu}{\partial N}\right)_{v_{(r)}} \quad ; \quad \omega^+ = \frac{\mu^2}{2\eta}$$

Eq. 3:

$$f_{(r)}^{+} = \left(\frac{\partial \rho_{(r)}}{\partial N}\right)_{v_{(r)}}^{+} \approx \left|\psi_{(r)\,\mathrm{LUMO}}\right|^2 = \rho_{(r)\,\mathrm{LUMO}}$$

Eq. 4:

$$f_{(r)}^{-} = \left(\frac{\partial \rho_{(r)}}{\partial N}\right)_{v_{(r)}}^{-} \approx \left|\psi_{(r)\,\mathrm{HOMO}}\right|^2 = \rho_{(r)\,\mathrm{HOMO}}$$

Eq. 5:

$$f_{(r)}^{(2)} = \left(\frac{\partial f_{(r)}}{\partial N}\right)_{v_{(r)}} \approx f_{(r)}^{+} - f_{(r)}^{-} = \rho_{(r)\,\mathrm{LUMO}} - \rho_{(r)\,\mathrm{HOMO}}$$

The global reactivity indices (mainly the chemical potential, μ) allow describing the tendency of electron density acceptor and donor, i.e., those species that behave as nucleophiles and electrophiles. In general, the electron density tends to move from the species presenting a higher chemical potential value (less negative) towards the one presenting a lower chemical potential [45]. In this particular case, it can be observed that it is the Nitrone derivative that "attacks" the OH· radical, a phenomenon contrary to that presented in the literature, in which it is the OH· radical that acts on the chemical species, as described in the Hydrogen abstraction phenomenon [46,47,48].

The low reactivity of the OH· radical can be similarly evidenced with the chemical hardness (η), which is higher compared to nitrone derivatives, which is consistent with the principle of maximum hardness (PMH), which describes that more reactive systems exhibit lower hardness [49].

Table 2. Global and local reactivity indices of the nitrone groups of hBNn derivatives.

Specie	Atom	$f_{(r)}^{-}$	$f_{(r)}^{+}$	$f_{(r)}^{(2)}$	μ / eV	η / eV	ω^+ / eV
hBN1	1 C	0.0788	0.0823	0.0035	-4.0076	3.2128	2.4994
	2 C	0.0235	0.0373	0.0139			
	3 C	0.0298	0.0321	0.0023			
	4 C	0.0724	0.0863	0.0139			
	5 C	0.0320	0.0426	0.0107			
	6 C	0.0270	0.0511	0.0241			
	11 C	0.0844	0.0722	-0.0122			
	12 C	0.0515	0.1096	0.0588			
	13 N	0.0462	0.1106	0.0644			
	14 N	0.1084	0.0521	-0.0560			
	15 O	0.2360	0.1171	-0.1188			
	16 C	0.0026	0.0077	0.0051			
	20 O	0.2631	0.1031	-0.1600			
	21 C	0.0022	0.0023	0.0001			
	22 C	0.0017	0.0043	0.0029			
	26 C	0.0008	0.0000	-0.0008			
	30 C	0.0012	0.0038	0.0026			
hBN2	1 C	0.0774	0.0892	0.0118	-4.1541	3.2605	2.6463
	2 C	0.0260	0.0364	0.0103			
	3 C	0.0262	0.0373	0.0111			
	4 C	0.0800	0.0831	0.0031			
	5 C	0.0280	0.0485	0.0206			
	6 C	0.0280	0.0482	0.0202			
	11 C	0.0912	0.0586	-0.0325			
	12 C	0.1035	0.0556	-0.0479			
	13 N	0.0445	0.1036	0.0590			
	14 N	0.0487	0.1083	0.0596			
	15 O	0.2549	0.1056	-0.1493			
	16 C	0.0008	0.0067	0.0059			
	20 O	0.2512	0.1031	-0.1481			
	22 C	0.0250	0.0105	-0.0145			
hBN3	1 C	0.0787	0.0845	0.0058	-4.1446	3.4684	2.4763
	2 C	0.0690	0.0883	0.0193			
	3 C	0.0080	0.0301	0.0222			
	4 C	0.0592	0.0629	0.0036			
	5 C	0.0110	0.0182	0.0072			
	6 C	0.0573	0.0827	0.0254			
	11 C	0.0714	0.0685	-0.0029			
	12 C	0.0610	0.1248	0.0639			
	13 N	0.0411	0.1170	0.0759			
	14 N	0.0426	0.0957	0.0531			
	15 C	0.0021	0.0082	0.0060			
	19 O	0.2280	0.1137	-0.1143			
	20 O	0.2576	0.0764	-0.1812			
	21 C	0.0052	0.0012	-0.0040			
hBN4	1 C	0.0690	0.0933	0.0243	-4.0201	3.4942	2.3125
	2 C	0.0758	0.0911	0.0164			
	3 C	0.0168	0.0202	0.0035			
	4 C	0.0479	0.0804	0.0325			
	5 C	0.0045	0.0264	0.0220			
	6 C	0.0660	0.0716	0.0056			
	11 C	0.0875	0.0821	-0.0054			
	12 C	0.1024	0.0483	-0.0541			
	13 N	0.0487	0.1115	0.0628			
	14 N	0.0378	0.1014	0.0636			
	15 C	0.0033	0.0008	-0.0025			
	16 O	0.2724	0.0930	-0.1794			
	17 O	0.2073	0.0911	-0.1162			
	18 C	0.0007	0.0058	0.0051			
OH ·					-6.045	7.9443	2.3772

On the other hand, the Fukui and Dual Descriptor indices allow describing the localized reacting sites. In this particular case, it can be observed graphically (Figure 4) that the OH· radical presents electrophilic tendencies by presenting a purple color, while the double bond of the nitrone presents nucleophilic characteristics. From Table 2 it can be evidenced the different local reactivities presented by the nitrones functional groups, which describes the attack tendency towards the OH· radical and the subsequent formation of a spin adduct.

*Corresponding author email: jose.munoz.e@ug.uchile.cl

Figure 4. Indices of local reactivity of nitrone derivatives and OH· radical. The purple lobes represent electrophilic features, whereas the green lobes represent local nucleophilic tendencies.

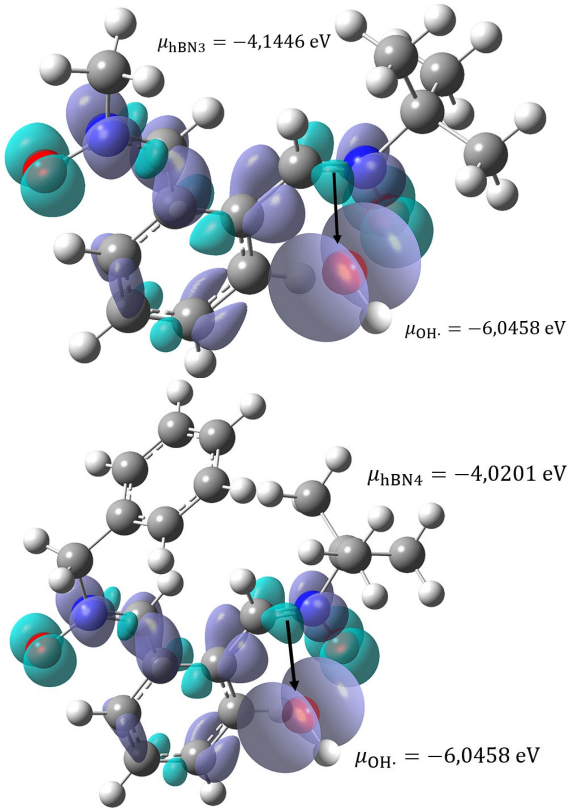

Compounds hBN1 and hBN3 exhibit higher nucleophilic reactivity on the 11 C atom (more sterically hindered carbon), whereas the nucleophilic reactivity of compounds hBN2 and hBN4 is centered on the 12 C atom (less sterically hindered carbon). Therefore, the mechanism of OH· radical trapping by the hBNn derivatives is given by the electronic transfer of the $N^+ = C$ double bond, to give way to a spin adduct with lower reactivity (Figure 5).

Figure 5. Mechanism of OH· radical trapping of hBNn nitrone derivatives.

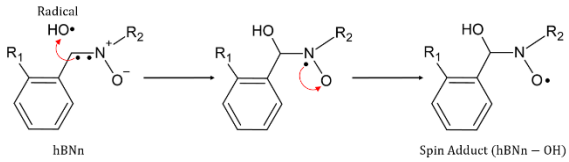

3.3. Natural Bond Orbital (NBO)

To describe and visualize the presence of delocalizations, non-bonding electronic pairs or Singly Occupied Molecular Orbital (SOMO) [50], the NBO method can be used, which are an intermediate electronic state between atomic orbitals (AO) and molecular orbitals (MO) [31].

Natural bonding orbitals (NBO) correspond to localized few-center bonds (one or two centers) that are formed by hybrid atomic orbitals (NHO), which allow describing the pattern of a molecular bond as a "Lewis diagram", i.e., it describes the bonding and non-bonding electron pairs of a molecule. Mathematically, a Natural Bond Orbital is described as the linear combination of Hybrid Atomic Orbitals (NHO) located between two atoms A and B.

$$\phi_{AB}^{NBO} = c_A \psi_A^{NHO} + c_B \psi_B^{NHO}$$

Being ϕ_{AB}^{NBO} the NBO orbital located between atoms A and B, cA and cB normalization constants (which are known as "polarization coefficients") indicating the nature of the bond, which can vary from covalent character $c_A = c_B$ to ionic character $c_A \gg c_B$ and ψ_A^{NHO}, ψ_B^{NHO} Hybrid Natural Orbitals. And in the same way as in molecular orbitals, for each bonding molecular orbital there is its respective anti-bonding orbital$\left(\phi_{AB}^{NBO^*}\right)$

$$\phi_{AB}^{NBO^*} = c_A \psi_A^{NHO} - c_B \psi_B^{NHO}$$

NBOs are localized orbitals that describe a Lewis-type structure, so in the context of NBOs the bonding orbitals $\left(\phi_{AB}^{NBO}\right)$ are referred to as "Lewis orbitals", on the contrary, the anti-bonding orbitals $\left(\phi_{AB}^{NBO^*}\right)$ are referred to as "non-Lewis orbitals".

The location of the radical electron corresponds to a non-bonding (n) NBO orbital, which is called SOMO, which could be studied and described in the literature [51]. The main contribution of this orbital corresponds to the Nitrone group, specifically to the N-O bond, where the radical electron is located, as can be seen in Fig. 5. Table 3 shows the non-bonding orbital contribution of each Nitrone group of the hBNn derivatives.

Table 3. Non-bonding character (n) of the SOMO of the spin adducts (notation: n: non-bonding, oc: occupied).

Specie	NBO (n)	Contribution	Specie	NBO (n)	Contribution
hBN1	67 (oc)	44.7% (N14)	hBN3	67 (oc)	43.5% (N14)
		38.6% (O20)			37.5% (O20)
		83.3% (n)			81% (n)
hBN2	75 (oc)	44.2% (N13)	hBN4	87 (oc)	43.8% (N13)
		40% (O15)			37.9% (O16)
		84.2% (n)			81.7% (n)

From Table 3 it can be seen that the radical electron localization presents a non-bonding character (SOMO) over 80% in each of the spin adducts, with the nitrogen atom of the Nitrone group contributing the most (>40%), while oxygen contributes the least (≤40%). The above can be visualized in Figure 6.

Figure 6 graphically depicts the SOMO generated by the hBNn-OH spin adduct after trapping of the OH·radical by the hBNn nitrone derivative.
In it, it can be seen how the electron radical is preferentially located on the N-O bond of the adduct, with a higher proportion on the nitrogen atom, as numerically described in Table 3.

Figure 6. NBO SOMO description of hBNn-OH spin adducts.

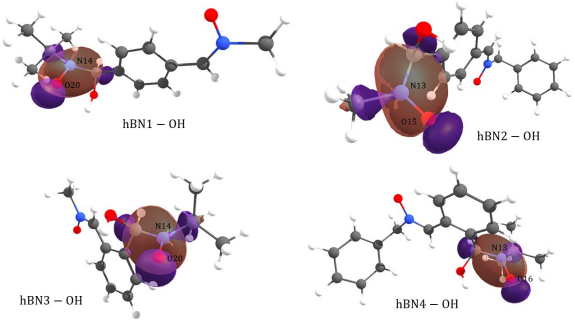

4. CONCLUSION

According to the results presented, it can be concluded that hBNn nitrone derivatives (PBN) show antioxidant OH· radical trapping capacity, forming thermodynamically stable spin adducts. From the global and local reactivity point of view, it could be observed that the reaction mechanism takes place between the OH· radical, which behaves as an electrophile, while the nitrones (specifically their double bond) behave as nucleophiles.

From the NBO analysis it was possible to characterize the SOMO of the spin adduct, locating the electron radical mainly between the nitrogen and oxygen atoms of the nitrone.

5. ACKNOWLEDGMENTS

Grateful thanks for the PIDi - UTEM high performance computing system (SCC - PIDi - UTEM CONICYT - FONDEQUIP - EQM180180) of the Universidad Tecnológica Metropolitana, Santiago, Chile, for providing the computational support computational support to perform the computational calculations. José Muñoz cordially thanks Ms. Vania Castillo (UNAB) for her suggestions in the correction and editing of this article. The article underwent a final proofreading review.

6. REFERENCES

1. Di V. Lobo, A. Patil, A. Phatak, & N. *Chandra. Pharmacognosy reviews*, 4(8), 118–126 (2010)
2. W. R. Markesbery & J. M. Carney. *Brain pathology (Zurich, Switzerland)*, 9(1), 133–146 (1990)
3. M. Aslan & T. Ozben. *Current Alzheimer research,* 1(2), 111–119 (2004)
4. M. Ebadi, S. K. Srinivasan, & M. D. *Progress in neurobiology*, 48(1), 1–19 (1996)
5. G. Perry, A. Nunomura, K. Hirai, X. Zhu, M. Pérez, J. Avila, R. J. Castellani, C. S. Atwood, G. Aliev, L. M. Sayre, A. Takeda & M. A. Smith, M. A. *Free radical biology & medicine,* 33(11), 1475–1479 (2002)
6. H. Kumar, H-W. Lim, SV. More, B-W. Kim, S. Koppula, IS Kim, D-K Choi. International *Journal of Molecular Sciences,* 13(8), 10478-10504 (2012)
7. N. Gupta, K. Verma, S. Nalla, A. Kulshreshtha, R. Lall, & S. Prasad. *Molecules (Basel, Switzerland)*, 25(22), 5390 (2020)
8. A. ipak Gašparović. Free Radical Research in Cancer. *Antioxidants (Basel, Switzerland),* 9(2), 157 (2020)
9. J. Krzemińska, M. Wronka, E. Młynarska, B. Franczyk & J. Rysz. *Antioxidants (Basel, Switzerland),* 11(1), 172 (2022)
10. U. Asmat, K. Abad, & K. Ismail. *Saudi pharmaceutical journal*: *SPJ*, 24(5), 547–553 (2016)
11. J.S. Johansen, A.K. Harris, D.J. Rychly et al. *Cardiovasc Diabetol*, 4, 5 (2005)
12. P.D. Ray, B.W. Huang, & Y. Tsuji. Cellular signalling, 24(5), 981–990 (2012)
13. M. C., Martínez & R. Andriantsitohaina, R. *Antioxidants & redox signaling*, 11(3), 669–702 (2009)
14. Qun Chen, Edwin J. Vazquez, Shadi Moghaddas, Charles L. Hoppel, Edward J. Lesnefsky. *Journal of Biological Chemistry*, 278 (38), 36027-36031 (2003)
15. I. V. Turko, S, Marcondes & F. Murad. Heart and circulatory physiology, 281(6), H2289–H2294 (2001)
16. A. Ayala, M. F. Muñoz & S. Argüelles. *Oxidative medicine and cellular longevity*, 360438 (2014)
17. D. A. Wink, R. W. Nims, J. E. Saavedra, W. E. Jr., Utermahlen & P. C. Ford. *Proceedings of the National Academy of Sciences of the United States of America*, 91(14), 6604–6608. (1994)
18. T. Ramasarma. *Current Science,* 92(2), 184–191 (2007)
19. S. E. Espinoza, H. Guo, N. Fedarko, A. DeZern, L. P. Fried, Q. L. Xue, S. Leng, B. Beamer & J. D. Walston, J. D. The journals of gerontology. Series A, *Biological sciences and medical sciences*, 63(5), 505–509 (2008)
20. A. Nandi, L. J. Yan, C. K. Jana & N. Das. Oxidative medicine and cellular longevity, 9613090 (2019)
21. J. Bouayed & T. Bohn. *Oxidative medicine and cellular longevity,* 3(4), 228–237 (2010)
22. N. Liang, D. D. *Kitts. Molecules,* 19(11), 19180-19208 (2014)
23. K. Bakhouche, Z. Dhaouadi, N. Jaidane & D. Hammoutène. *Computational and Theoretical Chemistry,* 1060, 58–65 (2015)
24. G. Barriga-González, C. Aliaga, E. Chamorro, C. Olea-Azar, E. Norambuena, W. Porcal, M. González & H. Cerecetto. *RSC advances,* 10(66), 40127–40135 (2020)
25. F. A. Villamena, C. M. Hadad, & J. L. Zweier, J. L. *Journal of the American Chemical Society,* 126(6), 1816–1829 (2004)
26. D. Hadjipavlou-Litina, I. E. Głowacka, J. Marco-Contelles, D. G. Piotrowska. *Antioxidants,* 12, 36 (2023)
27. D. Iriepa, I. López-Muñoz, F. Marco-Contelles, J., Hadjipavlou-Litina. *Antioxidants,* 11, 1575 (2022)
28. R. A. Floyd, R. D. Kopke, C. H. Choi, S. B. Foster, S. Doblas & R. A. Towner. *Free radical biology & medicine*, 45(10), 1361–1374 (2008)
29. R. G. Parr, W. Yang. *Journal of the American Chemical Society,* 106, 4049 – 4050 (1984)
30. C. Morell, A. Grand, A. Toro-Labbé. *Journal of Physical Chemistry A*, 109, 205–212 (2005)
31. E.D. Glendening, C. R. Landis, F. Weinhold. *Wiley Inter-disciplinary Reviews: Computational Molecular Science,* 2(1), 1 – 42 (2011)
32. M. J. Frisch, G. W. Trucks, H. B. Schlegel, G. E. Scuseria, M. A. Robb, J. R. Cheeseman, G. Scalmani, V. Barone, B. Mennucci, G. A. Petersson, H. Nakatsuji, M. Caricato, X. Li, H. P. Hratchian, A. F. Izmaylov, J. Bloino, G. Zheng, J. L. Sonnenberg, M. Hada, M. Ehara, K. Toyota, R. Fukuda, J. Hasegawa, M. Ishida, T. Nakajima, Y. Honda, O. Kitao, H. Nakai, T. Vreven, J. A. Montgomery, Jr., J. E. Peralta, F. Ogliaro, M. Bearpark, J. J. Heyd, E. Brothers, K. N. Kudin, V. N. Staroverov, R. Kobayashi, J. Normand, K. Raghavachari, A. Rendell, J. C. Burant, S. S. Iyengar, J. Tomasi, M. Cossi, N. Rega, J. M. Millam, M. Klene, J. E. Knox, J. B. Cross, V. Bakken, C. Adamo, J. Jaramillo, R.

*Corresponding author email: jose.munoz.e@ug.uchile.cl

Gomperts, R. E. Stratmann, O. Yazyev, A. J. Austin, R. Cammi, C. Pomelli, J. W. Ochterski, R. L. Martin, K. Morokuma, V. G. Zakrzewski, G. A. Voth, P. Salvador, J. J. Dannenberg, S. Dapprich, A. D. Daniels, Ö. Farkas, J. B. Foresman, J. V. Ortiz, J. Cioslowski, and D. J. Fox, Gaussian 09, Revision E. 01, Gaussian, Inc., Wallingford CT. (2013)

33. M. A. Allodi, K. N. Kirschner & G. C. Shields. *The journal of physical chemistry A*, 112(30), 7064–7071 (2008)
34. M-J. Lee, B-D. Lee. Applied Sciences, 12(5), 2479 (2022)
35. R. Contreras, P. Fuentealba, M. Galván, P. Pérez. *Chemical Physical Letter*, 304(5-6), 405-413 (1999)
36. P. Fuentealba, P. Pérez, R. Contreras. *Journal of Chemical Physics*, 113(7), 2544-2551 (2000)
37. K. Fukui, T. Yonezawa & H. Shingu. *The Journal of Chemical Physics*, 20(4), 722–725 (1952)
38. I. Fleming. *Molecular orbitals and reactions of organic chemistry.* 1st Edition. Wiley Publishing House. Chap. 3, 2004; pp. 127 – 143.
39. F. Weinhold. *Journal of computational chemistry*, 33(30), 2363–2379 (2012)
40. E. Glendening, J. Badenhoop, A. Reed, J. Carpenter, C. Bohmann, C. Morales, C. Landis, F. Weinhold. *Journal of Computational Chemistry*, 34(16), 1429 – 1437 (2013)
41. G. A. Zhurko and D. A. Zhurko, *"ChemCraft, Tool for Treatment of the Chemical Data." http://www.Chem craft prog.com*
42. Y. Yamazaki, J. Naganuma & H. Gotoh. *Scientific reports,* 9(1), 20339 (2019)
43. R. G. Parr, W. Yang. *Density – Functional Theory of Atoms and Molecules*. Oxford University Press, USA Chap. 4 – 5 1994; 70 – 104
44. P. Geerlings, F. De Proft & W. *Langenaeker. Chemical Reviews*, 103(5), 1793–1874 (2003)
45. A. K. Chandra, M. T. Nguyen. *International Journal of Molecular Sciences*, 3(4), 310-323 (2002)
46. J. Moc & J. M. Simmie. *The Journal of Physical Chemistry A*, 114(17), 5558–5564 (2010)
47. A. M. Priya & S. Lakshmipathi. *Journal of Physical Organic Chemistry*, 30(12), e3713 (2017)
48. A. K. Chandra, T. Uchimaru, M. Sugie, & A. Sekiya. *Chemical Physics Letters*, 318(1-3), 69–74 (2000)
49. R. G. Pearson. *Chemical Hardness: Applications from Molecules to Solids, Wiley-VCH Verlag GMBH: Weinheim*. Chapter 4, 1997; pp. 99-124
50. IUPAC. Compendium of Chemical Terminology (the "Gold Book"), 2nd ed.; McNaught, A. D., Wilkinson, A., Eds.; Blackwell Scientific Publications: Oxford, 2017. *http://goldbook.iupac.org/AT06996.html*
51. A. Kumar & M. D. Sevilla. *The journal of physical chemistry. B*, 122(1), 98–105 (2018)